Analysis, design and techno-economic assessment of a base isolated steel building

Varnavas Varnava & Petros Komodromos
Department of Civil and Environmental Engineering, University of Cyprus

SUMMARY:
Seismic isolation is an effective method for the seismic protection of buildings. However, its adoption is often limited due to financial considerations. In this research work, the response of a steel building, considered as both base isolated and conventionally supported, under earthquake excitations is investigated taking into account the respective erection cost of either case. In addition, the base-isolated building is subjected to higher magnitude earthquakes than the design basis earthquake, in order to determine the size of the required seismic gap, which is compared with approximate methods for its calculation, provided by building codes. Furthermore, the accuracy of Eurocode 8 method for the linearization of isolator properties is studied. It is concluded that the usage of seismic isolation increases the cost of the structure, though it drastically improves its seismic response. Furthermore, the usage of a nonlinear model for the isolation system is found to be necessary in order to achieve a sufficiently accurate computation of the structural response and estimation of the width of the seismic gap.

Keywords: Seismic isolation, base isolation, seismic protection, linearization, seismic isolation cost

1. INTRODUCTION

Base or seismic isolation is an innovative design approach, used for the minimization of earthquake induced loads and the avoidance of damage in relatively stiff buildings. The method is based on the decoupling of a structure from the horizontal components of a ground motion, by the insertion of flexibility at the isolation level, and the avoidance of resonance, as the fundamental frequencies of the structure are shifted away from the predominant frequencies range of common earthquakes. The interstory deflections, floor accelerations and shear forces can be significantly reduced, while structural and non-structural damage can be avoided (Naeim and Kelly, 1999; Komodromos, 2000). The two main categories of seismic isolation systems are the elastomeric bearings and the friction-sliding systems. The elastomeric bearings are subdivided in the Natural Rubber Bearings (NRBs), the High Damping Rubber Bearings (HDRBs) and the Lead Rubber Bearings (LRBs) (Higashino and Okamoto, 2006). The NRBs provide necessary horizontal stiffness to the structure, but their energy dissipation capacity is usually insufficient, since their damping is limited in the range 2-3% of the critical viscous damping (Kelly, 2001). Thus they are generally used in combination either with HDRBs or LRBs, or with additional damping devices, necessary for the provision of adequate supplemental damping to the structure.

Since seismic isolation is commonly used for the seismic protection of high importance structures and rarely for residential buildings, mainly due to financial considerations, it is important to investigate and quantify the additional cost of seismic isolation in typical low-rise residential buildings and assess their seismic performance. The present paper examines the response of a base-isolated, two-story, steel residential building comparatively with an identical, conventionally based building, subjected to various earthquake excitations. While both structures are designed in order to fulfill the provisions of the Eurocodes and exhibit the same performance level, which is an equal maximum interstory deflection of the first story, a preliminary cost estimation is carried out. Furthermore, a few others aspects of the behavior of the base-isolated structure are investigated. The NRBs are characterized by essentially linear behavior and viscous damping mechanism (Skinner et al, 1993), while the LRBs exhibit non-linear hysteretic behavior. The linearization of the LRBs' behavior, which is allowed by Eurocode 8, under certain conditions, is not always an adequately accurate approach (Komodromos, 2000). In order to evaluate the accuracy of the linearization of the LRBs' properties, non-linear time-history analyses are performed, using the hysteretic Bouc-Wen constitutive model. Moreover, the simulated base-isolated structure is subjected to higher magnitude earthquakes than the design basis earthquake (DBE), so as to determine the size of the required seismic gap and assess the appropriateness of the proposed, by the Eurocode 8 and the Uniform Building Code 1997 (UBC 1997), methods for the preliminary calculation of the width of the required seismic gap.

2. RESEARCH OBJECTIVES AND SCOPE

2.1. Shear behavior and modeling of lead rubber bearings

The nonlinear hysteretic shear behavior of LRBs can be described by an inelastic bilinear model, characterized by the high initial elastic stiffness, K_{el}, the low post-yield stiffness, K_{py}, the yield force and displacement, F_y and U_y, respectively, the characteristic strength, Q, and the maximum force and displacement, F_d and U_d, respectively (Fig. 2.1). Although the bilinear model describes sufficiently well the accuracy of the shear behavior of LRBs, it incorporates a sudden transition from the elastic to the post elastic branch. The Bouc-Wen model, proposed by Wen (1976) and Park et al (1986) and recommended for base-isolation analysis by Nagarajaiah et al (1991), ensures a smooth transition between the two branches, as it is shown by the dashed curves in Fig. 2.1, has been implemented in various engineering applications (Charalampakis and Koumousis, 2008) and is commonly used for the simulation of LRBs' behavior (Wu et al, 2008; Providakis, 2008).

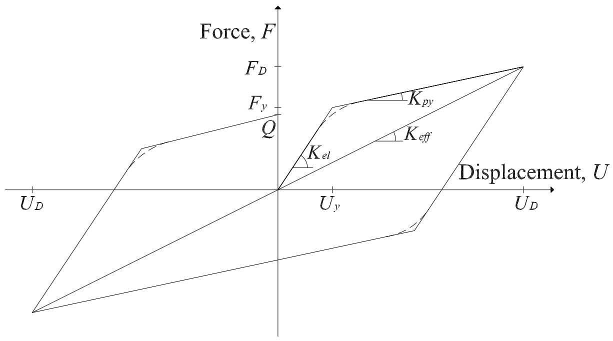

Figure 2.1. Inelastic shear behavior constitutive law of LRB.

In practice, equivalent linear elastic models are often used in order to further simplify the design and analysis of seismically isolated buildings, at least at the preliminary design and analysis phases. According to Eurocode 8, the seismic isolation system, under certain limitations, can be modeled using an equivalent linear viscoelastic behavior, based on an effective stiffness, K_{eff}, and an effective viscous damping ratio, ξ_{eff}, of the isolation system (Eqns. 2.1 & 2.2). Thus, it is very important to investigate the appropriateness of using such a linearized model, by comparing its computed responses with those of the more accurate Bouc-Wen model. Equations 2.3 & 2.4 are used to derive expressions for the calculation of the effective stiffness, $K_{effisol}$, and the effective damping, $\xi_{effisol}$, of the isolation system, since the isolation system under consideration is composed of both LRBs and NRBs.

$$K_{eff} = K_{py} + \frac{Q}{U_D} \tag{2.1}$$

$$\xi_{eff} = \frac{4Q(U_D - U_y)}{2\pi K_{eff} U_D^2} \tag{2.2}$$

$$K_{effisol}=\sum_{i=1}^{n}K_{effNRBi}+\sum_{j=1}^{m}K_{effLRBj}=\sum_{i=1}^{n}K_{rbi}+\sum_{j=1}^{m}\left(K_{pyj}+\frac{Q_j}{U_{Dj}}\right) \quad (2.3)$$

$$\xi_{effisol}=\frac{W_{DLRBs}+W_{DNRBs}}{2\cdot\pi\cdot K_{effisol}\cdot U_D^2}=\frac{4\cdot\left(\sum_{j=1}^{m}Q_j\right)\cdot(U_D-U_y)+2\cdot\pi\cdot\left(\sum_{i=1}^{n}K_{rbi}\right)\cdot\xi_{effNRB}\cdot U_D^2}{2\cdot\pi\cdot K_{effisol}\cdot U_D^2} \quad (2.4)$$

Where:
$K_{effNRBi}$, $K_{effLRBi}$: Effective stiffness of a NRB and a LRB isolator, respectively
K_{rbi}: Rubber stiffness of a NRB isolator
n, m: Number of NRB and LRB isolators respectively
W_{DNRBs}, W_{DLRBs}: Energy dissipated through a loading, unloading and reloading cycle, from the NRBs and the LRBs, respectively
ξ_{effNRB}: Equivalent viscous damping ratio of a NRB isolator (≈2 %)

Dicleli and Buddaram (2007) evaluated the equivalent linear elastic analysis for SDOF systems, concluding that the linearized model underpredicted the design displacement using the existing effective viscous damping ratio. Matsagar and Jangid (2004) analyzed the influence of isolator characteristics on the seismic response of base-isolated structures modeled as MDOF, suggesting that equivalent linear elastic models underestimate the superstructure accelerations and overestimate the design displacements. Mavronicola & Komodromos (2011) investigated the appropriateness of various literature-proposed relationships for the linearization of stiffness and the conversion of hysteretic to equivalent viscous damping of LRBs, concluding that usage of the proposed relationships results in overestimation of the maximum relative displacements at the isolation level and leads to large response discrepancies in comparison with those computed by the more accurate bilinear model.

2.2. Determination of the required width of the seismic gap

Between a seismically isolated structure and the surrounding structures a sufficient clearance, called seismic gap, should be provided in order to accommodate the large horizontal relative displacements that are expected at the isolation level. Chapter 10 of Eurocode 8-1 provides a methodology for the calculation of the required seismic gap, which takes explicitly into account the accidental torsional displacements of the isolation system. Moreover, in the Appendix Chapter 16 of UBC 1997, it is stated that the total design displacement and the total maximum displacement, thus the maximum displacement under the maximum credible earthquake, should comprise the additional displacement due to actual and accidental torsion calculated considering the spatial distribution of the lateral stiffness of the isolation system and the most disadvantageous location of mass eccentricity. The appropriateness of the two design codes' methodologies is assessed in comparison with the calculated displacements derived from linear and nonlinear analyses, for 3 different levels of peak ground acceleration (PGA) of the induced earthquake excitations.

2.3. Structural failures under high magnitude earthquakes

The superstructure of a seismically isolated building is designed to remain in the elastic range under earthquake excitations with equal or relevant magnitude with the DBE. However, since it would be interesting to explore potential failures and their mechanisms, under stronger excitations than the DBE, potential failures are also determined under two levels of PGA, 0.40 and 0.50 g, while the influence of the modeling of the LRB's - linearized or nonlinear Bouc-Wen constitutive law - on the range of failures is assessed.

3. STRUCTURAL ANALYSIS

3.1. Structural system and isolation system

The building under consideration is a 2 story dwelling located in a region in Cyprus, where the design ground acceleration is 0.25 g and the foundation soil is type B, according to Eurocode 8. The superstructure's members are made of hot-rolled steel, grade S275, and the floor slabs are composite with high-strength trapezoidal steel sheets. The raft foundation is made out of reinforced concrete with concrete class C25/30 and S500 grade reinforcing bars. The building is regular in plan and elevation, with 24 m x 20 m plan dimensions and 3.3 m story height. The lateral force resisting system of the principal *X*-direction is moment resisting frame. As shown in Fig. 3.1 the structural system of the outer frames of the secondary *Y*-direction is plain frame with pin-based columns and pin-ended tie beams. The outer frames of the *Y*-direction are equipped with x-diagonal braces on the edge bays. For the design of the hybrid isolation system, consisting of 14 NRBs and 6 LRBs, a target fundamental period, T_{dtar}, of 1.20 sec and an effective viscous damping ratio of 15 % have been assumed.

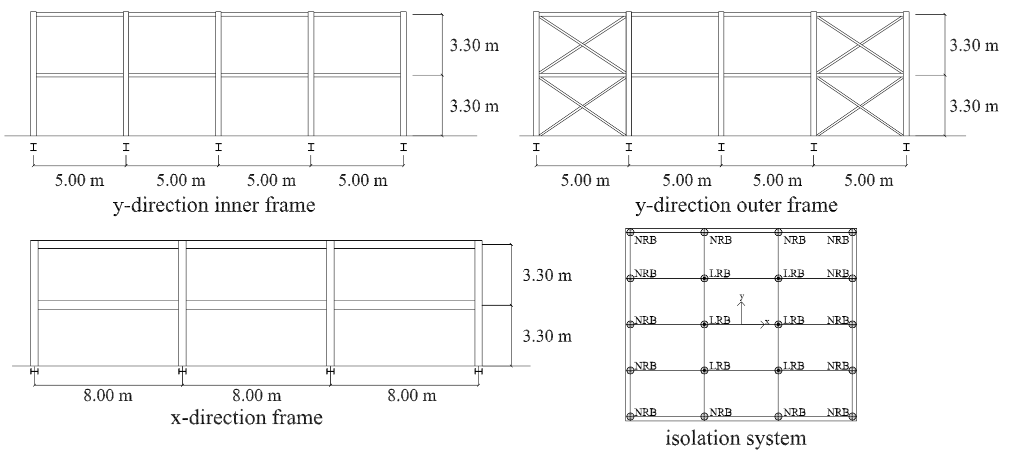

Figure 3.1. Structural and isolation systems.

3.2. Methodology and earthquake excitations

Seven pairs of accelerograms, consisting of *X-Y* components (Table 3.1.), are selected for the time-history analyses of the of the conventionally based structure (CBS) and the seismically isolated structure (SIS), which are performed using SAP2000 software. The accelerograms are scaled for 3 levels of PGA; 0.30, 0.40 and 0.50 g. Four load patterns are considered, thus the dead load, *G*, the live load, *L*, the earthquake action along the *X* direction, E_x, and the earthquake action along the *Y* direction, E_y while the structural response is obtained for 4 load combinations; one for the serviceability limit state and three for the ultimate limit state (Table 3.2.).

Table 3.1. Earthquake motions.

Earthquake	Date	Station	Components
Kalamata	13/09/1986	OTE- Building	N10W / N80E
Athens	07/09/1999	Sepolia (Garage)	LONG / TRAN
Ionian	04/11/1973	Lefkada OTE- Building	E-W / N-S
Thessalonika	20/06/1978	Thessaloniki-City Hotel	E-W / N-S
Kocaeli	17/08/1999	Duzce-Meteoroloji Mudurlugu	SN / WEST
Northridge	17/01/1994	Sylmar - County Hospital Parking Lot	1:90 Deg / 3:360 Deg
Parkfield	27/06/1966	Cholame Shandon	N85E / N05W

Table 3.2. Load Combinations.

Load Combination	Combined Actions
LC_1:	$1.00G + 1.00Q$
LC_2:	$1.35G + 1.50Q$
EC_1:	$1.00G + 0.30Q+1.00E_x+0.30E_y$
EC_2:	$1.00G + 0.30Q+0.30E_x+1.00E_y$

The differential equations of motion are solved with the Newmark (β=0.25, γ=0.50) direct integration method. The design of the two structures is based on a set common performance level, thus the equal maximum relative displacement of the first story of the two structures, under the DBE. Identification of failures and structural optimization is carried out by performing design checks, according to the provisions of Eurocode 3, which are incorporated in SAP2000.

4. ANALYSES RESULTS

4.1. Modal analysis

Base isolation shifts the fundamental period of the building from 0.212 s to 1.292 s. Since the ratio of the fundamental period of the seismically isolated structure (SIS) to the fundamental period of the conventionally based structure (CBS) is greater than 3, the torsional amplifications are limited and the ductility demand of the corner isolators is reduced (Tena-Colunga and Escamilla-Cruz, 2007). Also the torsional to lateral frequency ratio, as defined in Kilar and Koren (2009), is greater than unity, which indicates that the SIS is torsionally restrained. Fig. 4.1 provides the first 3 modes of the SIS and the CBS, while Table 4.1. provides the corresponding modal participation factors, indicating the significance of the predominant modes of the SIS.

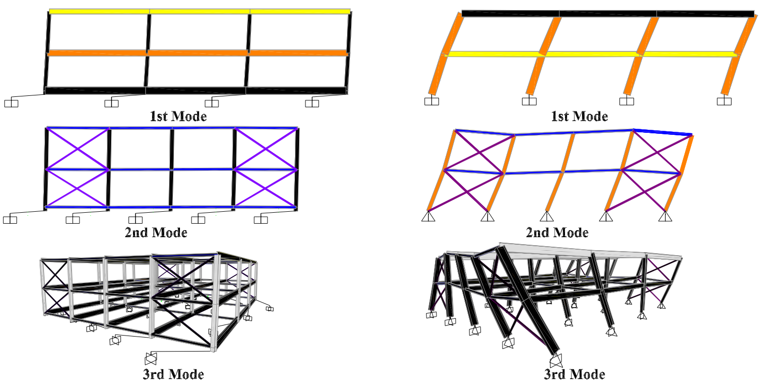

Figure 4.1. Fundamental modes of the SIS and CBS

Table 4.1. Fundamental eigenperiods and participation factors of CBS and SIS.

	Mode	Period (sec)	Modal Participating Mass Ratios U_x (%)	U_y (%)	R_z (%)
CBS	1	0.212	85.2	0	24.5
	2	0.151	0	93.0	38.5
	3	0.116	0	0	27.2
SIS	1	1.292	99.8	0	28.9
	2	1.267	0	100.0	41.7
	3	1.221	0	0	29.3

4.2. Interstory deflections

Fig. 4.2(a) shows that the 1st story of the structures under the two different configurations, CBS and the SIS, develops its maximum relative displacement along the *X* direction, with 0.60 and 0.62 cm, respectively. However, the SIS maximum relative displacement along the *Y* direction exceeds by 17.1% the corresponding displacement of the CBS. A significant reduction of the maximum relative displacement of the 2nd story of the SIS along *X* direction is gained, since it is reduced by 48% in comparison with the respective displacement of the CBS. Along the *Y* direction, the 2nd story of the SIS exhibits 16 % greater maximum relative displacement than the CBS. Generally, the CBS presents slightly smaller displacements along the *Y* direction, due to the required larger columns and the bigger braces, which are very effective in the reduction of the interstory deflections. Despite, the fact that the isolation system develops 8.30 and 13.54 cm displacements along the *X* and *Y* directions, respectively, that's not an issue of concern, since the seismic isolators can accommodate such strains.

While base isolation minimizes the interstory deflections due to the almost rigid body motion of the superstructure, the lateral load resisting system of the CBS had to be strengthened in order to reduce the interstory deflections to targeted levels. For this reason, HEB 600 and CHS 168.3x12.5 are used for the CBS column sections and brace sections, respectively, instead of HEA 300 and CHS 139.7x5, which are used for the SIS. Moreover, HEA 450 and IPE 550 are used for the major beams of the first and second story, respectively, of the CBS, while IPE 500 and IPE 400 are used for the SIS.

4.3. Floor accelerations

As shown in Fig. 4.2(b), seismic isolation drastically reduces the maximum floor accelerations of the building. On the contrary, the required stiffness increase in the case of the CBS, in order to limit its interstory deflections, amplifies substantially the absolute floor accelerations. Specifically, the diaphragm of the 1st story of the CBS develops approximately equal maximum absolute acceleration along the two principal, horizontal directions which are about 2.15 times greater than the PGA. The accelerations are amplified further on the 2nd story and they become 4.0 and 3.6 times greater than PGA, along the *X* and *Y* directions respectively. The absolute increase of the accelerations is more pronounced between the 1st and 2nd floors, rather than between the base and the 1st floor. The distribution of the maximum absolute accelerations developed on the diaphragms of the SIS is approximately orthogonal, which indicates that negligible amplification of the accelerations is taking place between the isolation diaphragm and the upper story. As it can be observed from Fig. 4.2(b), along the *X* direction, the accelerations of the diaphragms are 25 % less than the PGA, though they exceed it by 23 % along the *Y* direction (Fig. 5(b)). This difference is mainly due to the variation of the stiffness of the structural systems in the two directions, as the contribution of the X-diagonal braces to the total stiffness of the *Y* direction structural system is substantial leading to unavoidable amplification of the corresponding floor accelerations.

4.4. Floor shear forces

The developed shear forces at the diaphragms of the SIS are substantially reduced, as shown in Fig. 4.2(c). The base, story 1 and 2 shear forces of the CBS along the *X* direction are 186, 337 and 434 % greater than the corresponding shear forces of the SIS, while along the *Y* direction they are 67, 156 and 222 % greater. It is remarkable that the base shear along the *X* direction of the SIS is less than the top floor shear of the CBS whereas along the *Y* direction is slightly bigger. Moreover, the interstory drift sensitivity coefficient, θ, was computed, according to paragraph 4.4.2.2(2) of Eurocode 8, indicating that the second order effects have negligible effect to the response of both structures.

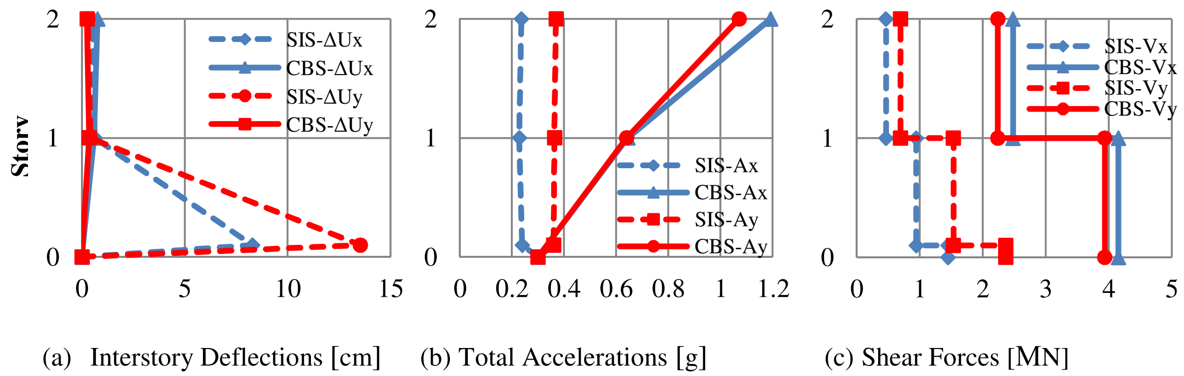

Figure 4.2. Envelope of: (a) maximum maximum interstory deflections, (b) absolute floor accelerations and (c) absolute maximum floor shear forces, along the *X* and *Y* directions under EC_1 and EC_2 combinations respectively.

4.5. Financial assessment

While the previous sessions demonstrate the beneficial contribution of base isolation to the seismic performance of the building, this section provides a brief summary of the additional economic cost for the implementation of seismic isolation. A noteworthy cost reduction of columns (58.3 %), braces (66.7 %), story 1 beams (31.8%), story 2 beams (32.4 %) and structural connections (40.6 %) is achieved in the SIS, as shown in Fig. 4.3. Although the construction cost of the SIS is raised by 30.1%, the cost of the isolators, which is about € 50,000, is almost counterbalanced by the savings in the cost of the aforementioned components. A significant cost shall be expended for the construction of the ground floor deck, which is required to act as an isolation diaphragm. The former consists of a grid of tie beams, supporting the composite slab and its total cost arises to about € 43,000.

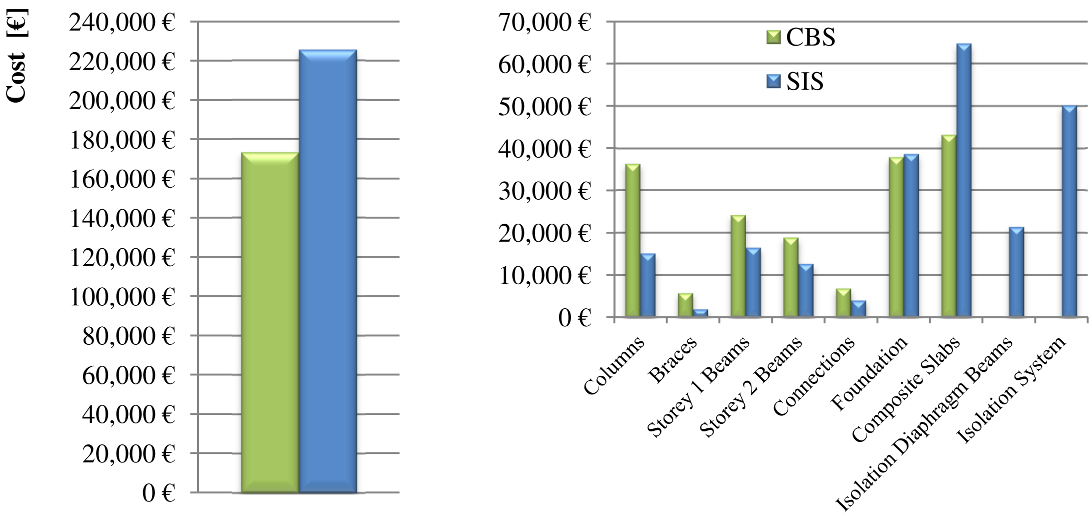

Figure 4.3. (a) Total construction cost (b) cost of major structural components of CBS and SIS.

4.6. Evaluation of the accuracy of LRB's linearized constitutive law

The use of the Bouc-Wen constitutive law for modeling the LRBs' shear behavior seems to have a rather insignificant effect on the displacements of the isolation system. The use of linear models leads to 1.3% overestimation of the maximum isolation system's displacement along the *X* direction and to 0.3% underestimation of the corresponding displacement along *Y* direction. However, the linearization of LRBs' behavior affects strongly the interstory deflections. The maximum interstory deflections of stories 1 and 2, along the *X* direction, are underestimated by 13.9 and 23.5 % respectively, whereas they are overestimated by 10.8 and 11.5 % along the *Y* direction (Fig. 4.4(a)).

Furthermore, Fig. 4.4(b) shows that the linear model exhibits minor relative errors on the computation of the maximum absolute accelerations of the isolation diaphragm and 1st story along the *X* direction. Contrarily, it leads to a tremendous underestimation of 27.8 % of second story's absolute acceleration, while an overestimation of the respective accelerations is noticed along the *Y* direction (Fig. 4.4(b)). A similar error of approximately -15 % is notated at the isolation diaphragm and 1st story accelerations, while the error is reduced at -13.2 % at the 2nd story. Another important observation is that the linear model yields an orthogonal height distribution of maximum accelerations, which is altered by the nonlinear model along the *X* direction. The particular distribution is probably caused due to the excitation of higher eigenmodes, which is a phenomenon that the linear model cannot capture.

The linear analyses exhibit an overestimation of the maximum base shear forces, 2.3 % along the *X* direction and more than 5 times greater (11.9 %) along the transverse direction (Fig. 4.4(c)). Story shear forces are significantly underestimated along the *X* direction and the relative error is increased by height. Specifically, it is equal to 11.8 % at the 1st and 25.7 % at the 2nd story. On the contrary, story shear forces are overestimated along *Y* direction and the relative error is not fluctuating much by height, since it is equal to -12.3 and –11.6 % at the 1st and 2nd story, respectively.

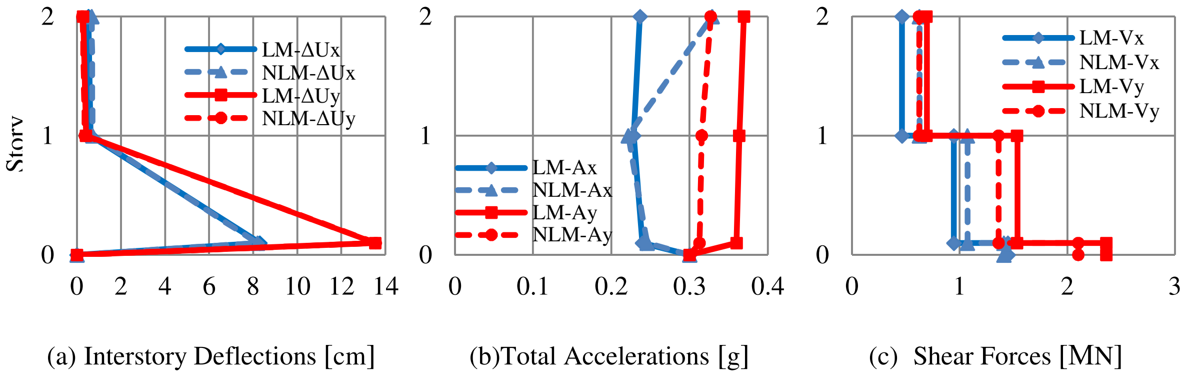

Figure 4.4. Envelope of (a) maximum interstory deflections, (b) maximum absolute floor accelerations and (c) maximum floor shear forces, along the *X* and *Y* directions under EC_1 and EC_2 combinations, respectively.

It can be concluded that the linearization of the LRBs' constitutive law yields a relatively accurate model of the response of the isolation system under the DBE. The detailed modeling of the LRBs' nonlinear behavior and their hysteretic energy dissipation mechanism, by the adoption of Bouc-Wen model, alters noticeably the response of the superstructure. However, a certain tendency could not be ascertained, since the modification of the response is different along the two principal directions and it would require a parametric analysis. The implementation of the linearized model leads to a conservative estimation of the SIS' response along the *Y* direction and insecure along the *X* direction. It is evident that for adequately accurate analysis and design of a SIS, isolated partially or entirely with LRBs', the nonlinear behavior of the seismic isolation system should be explicitly modeled.

4.7. Structural failures under high magnitude earthquakes

Under the selected earthquakes scaled to a 0.40 g PGA, linear analyses demonstrate failure of all braces and eight columns of the 1st story, while the usage of the nonlinear model (NLM) limits the failures only at the 1st story braces (Fig. 4.5). These failures occurred only under the action of the major seismic component of the Kocaeli excitation along the *Y* direction. If the linear model is implemented, all of the 1st story columns and braces and the half of the 2nd story braces fail under excitations with a PGA 0.50 g. The analyses using the NLM indicate failure of all the braces and 14 columns of the 1st story. The failure mechanism of braces is axial buckling, while the columns are damaged due to biaxial moment and axial force interaction. It should be noted, that failures developed, only when the major seismic component acts along the *Y* direction, under Kocaeli and Northridge pairs of excitations.

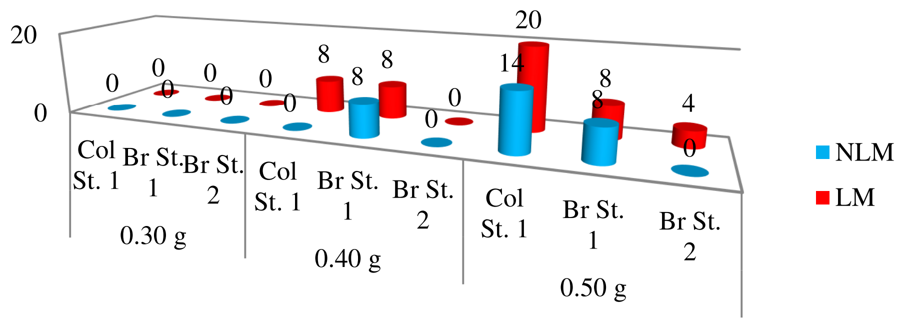

Figure 4.5. Failures of superstructure's members under 3 levels of earthquake magnitude, by adopting nonlinear (NLM) and linearized (LM) constitutive laws for modeling of LRBs' behavior.

4.8. Determination of the size of the seismic gap

The width of the seismic gap has been determined according to the methodologies of Eurocode 8 and UBC 1997, for 3 levels of earthquake magnitude (Table 4.2.). Under higher magnitude earthquakes than the DBE, the effective stiffness of the isolation system decreases. This results in the increase of the energy that is dissipated from the isolation system through a loading, unloading and reloading cycle, while its equivalent viscous damping ratio ξ_{eff} is reduced. This reduction is the product of the significant decrease of the LRBs' ξ_{eff} and the minor increase of NRBs' ξ_{eff}.

The maximum displacements of the isolation system along the two principal directions and the calculated sizes of the seismic gap are presented in Fig. 4.6. It is obvious that Eurocode 8 yields greater total displacements, since the displacements are multiplied with a magnification factor equal to 1.2, although the additional displacements due to accidental torsion are less. Both design codes' methodologies provide a secure estimation of the displacements along the *X* direction, but they yield unsecure results for the transverse direction. Another important outcome is that as the earthquake magnitude increases, the linear model becomes more conservative for the estimation of maximum displacement of the isolation system, along the *Y* direction. It is demonstrated that the considered methodologies can be used for the preliminary estimation of the size of the clearance. The performance of nonlinear analyses is considered necessary for the accurate determination of the size of the seismic gap in order to prevent the catastrophic effects of potential structural pounding.

Table 4.2. Violations of seismic gap by linear and nonlinear model.

	Maximum percentage exceedance :					
	Eurocode 8			UBC 1997		
PGA	Gap (cm)	LM	NLM	Gap (cm)	LM	NLM
0.30 g	10.76	25.8 %	26.2%	9.31	45.4 %	45.9%
0.40 g	16.24	34.5 %	24.9 %	14.15	54.4 %	43.3 %
0.50 g	22.49	40.6 %	20.6 %	19.67	60.7 %	37.9 %

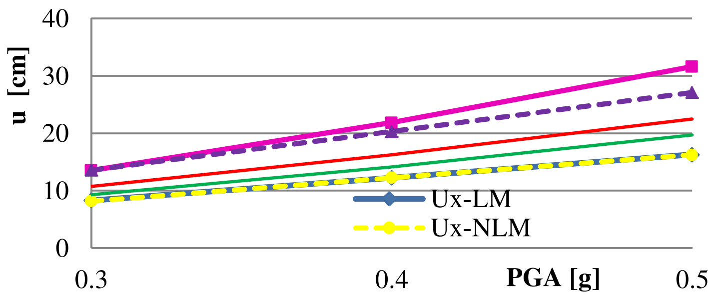

Figure 4.6. Maximum isolation displacement along two principal directions, under 3 levels of PGA.

5. CONCLUSIONS

Base isolation has been proved an efficient method for a substantial reduction of the interstory deflections, the maximum floor accelerations and the floor shear forces of the steel building under consideration. Despite the significant cost savings from the structural members, which almost counterbalance the cost of the isolation system, the total cost of the SIS is raised by about 30 %, mainly due to the cost of the required isolation diaphragm. The linearization of the shear behavior of the LRBs results in significant errors in the computation of superstructure's response, although it is relatively accurate for the isolation system's response. The use of a linearized model shall be restricted in the preliminary analysis phase, since it yields, in some cases, insecure results. The implementation of the Bouc-Wen model is considered necessary for both analysis and design purposes, while the estimation of the required width of the seismic gap should be based on nonlinear analyses.

REFERENCES

Charalampakis, A.E. and Koumousis, V.K. (2008). On the response and dissipated energy of Bouc–Wen hysteretic model. *Journal of Sound and Vibration* **309**,887-895.

Dicleli, M. and Buddaram, S. (2007). Comprehensive evaluation of equivalent linear analysis method for seismic-isolated structures represented by sdof systems. *Journal of Engineering Structures* **29**,1653-1663.

Higashino, M. & Okamoto, S. (2006). Response control and seismic isolation of buildings, Taylor & Francis Oxon, U.K.

Kelly, T. E. (2001). Base isolation of structures. Design Guidelines, Holmes Consulting Group, Wellington, New Zealand.

Kilar, V. and Koren, D. (2009). Seismic behaviour of asymmetric base isolated structures with various distributions of isolators. *Engineering Structures* **31**,910-921.

Komodromos, P. (2000). Seismic isolation for earthquake resistant structures, WIT Press, Southampton, U.K.

Matsagar, V.A. and Jangid, R.S. (2004). Influence of isolator characteristics on the response of base-isolated structures. *Engineering Structures* **26**,1735–1749.

Mavronicola, E. and Komodromos, P. (2011). Assessing the suitability of equivalent linear elastic analysis of seismically isolated multi-storey buildings. *Computers and Structures* **89**,1920-1931.

Naeim, F. and Kelly, J.M. (1999). Design of seismic isolated structures. From theory to practice, John Wiley & Sons INC, California, U.S.A.

Nagarajaiah, S., Reinhorn, A.M. and Constantinou, M.C. (1991). Nonlinear dynamic analysis of 3-D base isolated. *Journal of Structural Engineering* **117:7**,2035-2054.

Park, Y.J., Wen, Y.K. and Ang, A. H-S. (1986). Random vibration of hysteretic systems under bi-directional ground motions. *Earthquake Engineering and Structural Dynamics* **14**,543-557.

Providakis, C.P. (2008). Pushover analysis of base-isolated steel–concrete composite structures under near-fault excitations. *Soil Dynamics and Earthquake Engineering* **28**,293–304.

Skinner, R.I., Robinson, W.H. and McVerry, G.H. (1993). An introduction to seismic isolation, John Wiley & Sons Ltd, West Sussex, U.K.

Tena-Colunga, A. and Escamilla-Cruz, J.L. (2007). Torsional amplifications in asymmetric base-isolated structures. *Engineering Structures* **29**,237–247.

Wen, Y.K. (1976). Method for random vibration of hysteretic systems. *Journal of Engineering Mechanics - ASCE* **102:2**,249-263.

Wu, C., Li, Y., Li, H. and Zhang, K. (2008). Parametric Study on Seismic Energy Response of Base-isolated Structures. *International Workshop on Modelling, Simulation and Optimization,WMSO 2008*. **Vol I:** 375-378.

EN 1993-1-1:2005. Eurocode 3: Design of steel structures - Part 1-1: General rules and rules for buildings. European Committee for Standardization, Brussels, Belgium.

EN 1998-1:2004. Eurocode 8: Design of structures for earthquake resistance - Part 1: General rules, seismic actions and rules for buildings. European Committee for Standardization, Brussels, Belgium.

Uniform Building Code (1997). Structural Engineering Design Provisions. International Conference of Building Officials, California, U.S.A.